

Single production of composite electrons at the future SPPC-based lepton-hadron colliders

A. Caliskan*

*Gümüşhane University, Faculty of Engineering and Natural Sciences,
Department of Physics Engineering, 29100, Gümüşhane, Turkey*

Abstract

We consider the production of excited electrons with spin-1/2 at the future SPPC-based electron-proton colliders with center-of-mass energies of 8.4, 11.6, 26.6 and 36.8 TeV. These exotic particles are predicted in the composite models. We calculate the production cross-sections and concentrate on the photon decay channel of the excited electrons with the process of $ep \rightarrow e^*X \rightarrow e\gamma X$. The pseudorapidity and transverse momentum distributions of the electrons and photons in the final-state have been plotted in order to determine the kinematical cuts best suited for discovery of the excited electrons. By applying these cuts we compute 2σ , 3σ and 5σ contour plots of the statistical significance of the expected signal in the parameter space (L, m^*) , where L denotes the integrated luminosity of the collider and m^* is the mass of the composite electrons.

*Electronic address: acaliskan@gumushane.edu.tr

I. INTRODUCTION

Elementary particles and electromagnetic, weak and strong interactions among them today are well described by the Standard Model (SM) in particle physics. Discovery of the Higgs boson with a mass of approximately 125 GeV by the ATLAS [1] and the CMS [2] collaborations in 2012 confirmed the electroweak symmetry breaking mechanism of the SM. This discovery has further increased the reliability and accuracy of the SM. But, the SM still contains many puzzles and will likely need some modifications in the future. Some of the main problems to be solved in the SM are the neutrino masses, quark-lepton symmetry, family replication, large number of free parameters, CP violation, fermion's masses and mixing pattern. The most powerful candidates that can solve these problems are theories beyond the SM that have been studied over the years. A lot of theory like Technicolour [3, 4], Grand Unified Models [5, 6] and Supersymmetry [7] are proposed so far, but the most important one is the compositeness [8] that better explains the proliferation of elementary particles, introducing new fundamental constituents called preons.

Lepton and quark compositeness were firstly proposed at the 1970s [9–12], and so far many preonic models claiming that quarks and leptons have a sub-structure are proposed. The most important ones of them are the Fritzsche-Mandelbaum model [13, 14] (the so-called haplon model), Harari-Shupe model [15, 16] (the so-called rishon model), Terazawa WCH model [9] and Abboth-Farhi [17] model. In the Fritzsche-Mandelbaum model, for example, leptons and quarks are bound states of four fundamental preons, two of which are fermionic and two are bosonic, called α, β, x and y . Possible new interactions between the fermions should occur at the scale of binding energies that connect the preons together. This energy scale is an important parameter for all composite models, and called compositeness scale, Λ .

As a consequence of the compositeness we expect that the SM leptons will have their excited states if they have a sub-structure. Therefore the excited leptons ($e^*, \mu^*, \tau^*, \nu_e^*, \nu_\mu^*, \nu_\tau^*$) are studied by the composite models. It is estimated that the masses of the excited leptons, which may have spin-1/2 or higher spin states, need to be heavier compared to the SM leptons.

In the literature there are important recent searches that have studied the production of excited leptons in various colliders and estimated mass limits for their discovery. Composite

majorana neutrinos [18] and doubly charged excited leptons [19, 20] have been studied in detail at the Large Hadron Collider (LHC) energies. When we look at the future colliders, the studies of excited neutrino production at the CLIC [21] and the LHeC [22] colliders, and excited muon [23] and neutrino [24] productions at the FCC-based future colliders have been performed. Although several theoretical and phenomenological studies have been carried out on the composite leptons, no evidence has yet been obtained about the existence of them in the experimental studies at the LEP [25], HERA [26], TEVATRON [27], ATLAS [28] and CMS [29].

The greatest benefit of the experimental studies is the exclusion of energy regions where there is no signal for the existence of the excited leptons, and consequently the determination of a lower mass limit for the subsequent studies. The most up-to-date experimental results for the excited electrons were obtained from the OPAL [30] and CMS [29] experiments carried out at the CERN. In the OPAL experiment, the pair production of the excited electrons was investigated by electron-positron collisions ($e^+e^- \rightarrow e^*e^*$), and the mass limit was determined as $m_{e^*} > 103.2$ GeV. The single production of the excited electrons ($pp \rightarrow ee^*X$) was searched for and the mass values up to 3900 GeV were excluded. These experimental mass limits for the excited leptons were obtained from the gauge interactions assuming $f = f' = 1$ and $\Lambda = m_{e^*}$.

In addition to gauge interactions, another production mechanism of the excited leptons are the four fermion contact interactions. It is known that the contact interactions contribute to the production of the excited leptons at a level comparable to their gauge interactions. In fact, in a recent phenomenological study on proton-proton collisions [18] it has been shown that the contact interactions predominate for the production of the excited leptons at the LHC energies. We have taken the gauge interactions into account for current work, but it is not true that we omit the contribution of the contact interactions altogether. So we have planned the contact interaction version of this work as the subject of a future study.

In this paper we have searched for the single production of the excited electrons at the Super Proton-Proton Collider (SPPC)-based electron-proton colliders including four different center-of-mass energy options. After a general introduction in this section, the rest of the paper is organised as follows: in Section 2 we discuss the SPPC-based electron-proton collider options and their general accelerator parameters; in Section 3 we present the excited electron interaction Lagrangian, its cross-sections and decay widths; in Section 4 we

do signal and background analysis to determine mass limits for discovery; finally Section 5 contains the final discussions and conclusions.

II. THE SPPC-BASED LEPTON-HADRON COLLIDERS

With discovery of the Higgs particle at the CERN particle physics has reached the Higgs era, but it is unclear whether this particle is a fundamental scalar. The next step to be done is that the properties of the Higgs particle should be examined in detail and the true internal structure should be understood. For this purpose, the feasibility studies have been initiated to establish a Higgs factory all over the world.

The LHC collider is the world's most powerful particle collider built to date. It is still in operation and will continue to operate until the 2030s as part of its high-luminosity upgrade programme. In order to examine primarily the properties of the Higgs particle, the design of various collider projects planned to be established in the future has been started. Some of them are categorized in the literature as the LHC era colliders. Important international collider projects in the LHC era are the ILC (International Linear Collider) with $\sqrt{s}=0.5(1)$ TeV [31], low energy muon collider ($\mu^-\mu^+$) [32], LHeC (Large Hadron Electron Collider) with $\sqrt{s}=1.3$ TeV [33] and CLIC (Compact Linear Collider) with $\sqrt{s}=3$ TeV (optimal) [34]. The design works of these international projects have reached a certain stage.

The most important collider project to be established in the Europe for the post-LHC era is the international Future Circular Collider (FCC) project [35]. The design works of the FCC, which will have a center-of-mass energy of 100 TeV, started at CERN in 2010-2013 and supported by the European Union within the Horizon 2020 Framework for Research and Innovation. The main purpose of the FCC project to be built in the 80-100 km new tunnel at the CERN is to install an energy-frontier hadron-hadron collider (FCC-hh) with $\sqrt{s}=100$ TeV. In the next phase of the project, it is also planned to establish a lepton-lepton collider (FCC-ee or TLEP [36]) with a center-of-mass energy of 90-400 GeV to the same tunnel. With the lepton collider being activated the lepton-hadron collider option (FCC-he) will be available as a third collider type. The FCC project will allow us to search for the Higgs particle and new interactions beyond the SM at the highest energies. The Conceptual Design Report (CDR) of the project has been written as four volumes in 2018 [37–40].

Another important collider project to be established in the post-LHC era is the CEPC-

Table I: The main parameter options of the proton beams for the SPPC collider.

| Parameters | Option-1 (Pre-CDR) | Option-2 | Option-3 (CDR) | Option-4 |
|---|--------------------|----------|----------------|----------|
| Beam energy (TeV) | 35.6 | 35 | 37.5 | 68 |
| Circumference (km) | 54.7 | 54.7 | 100 | 100 |
| Dipole field (T) | 20 | 19.69 | 12 | 20.03 |
| Peak luminosity ($\times 10^{35} cm^{-2} s^{-1}$) | 1.1 | 1.2 | 1 | 10.2 |
| Particle per bunch (10^{11}) | 2 | 2 | 1.5 | 2 |
| Norm. transverse emittance (μm) | 4.1 | 3.72 | 2.4 | 3.05 |
| Bunch number per beam | 5835 | 5835 | 10080 | 10667 |
| Bunch length (mm) | 75.5 | 56.5 | 75.5 | 15.8 |
| Bunch spacing (ns) | 25 | 25 | 25 | 25 |

SPPC collider. The CEPC-SPPC which was started to be designed by Chinese physicists in 2012 is a two-stage circular collider project. Its Preliminary Conceptual Design Report (Pre-CDR) was completed in 2015 [41] and the CDR of the project was published in 2018 as two volumes [42, 43]. In the first stage of the project according to this reports, an electron-positron collider, called the Circular Electron Positron Collider (CEPC), with a center-of-mass energy of 240 GeV will be install to investigate primarily the Higgs physics in a 100 km tunnel. After the CEPC collider completes its missions it will be upgraded to the second stage. In the second stage an energy-frontier hadron-hadron collider, called Super Proton Proton Collider (SPPC), with a center-of-mass energy of more than 70 TeV will be installed in the same tunnel. Although the center-of-mass energy of the SPPC collider is about 70 TeV according to the Pre-CDR, this value was increased to 75 TeV in the CDR report. But, the ultimate goal of the project is to reach higher center-of-mass energy levels. Table 1 denotes the general parameters reported in the Pre-CDR and CDR of the SPPC collider, including various design options [44].

A lepton-hadron collider option can be obtained if a linear electron accelerator is installed tangentially to the SPPC proton complex. It is important here that the electron accelerator is linear because it is more difficult to reach higher energies due to synchrotron radiation in the circular electron accelerators. In the reference [45], four types of electron proton colliders have been recently proposed by using the parameters of known linear electron

Table II: The main parameters of the SPPC-based lepton-hadron colliders.

| Colliders | $E_e(\text{TeV})$ | $E_p(\text{TeV})$ | $\sqrt{s}(\text{TeV})$ | $L_{int}(\text{cm}^{-2}\text{s}^{-1})$ |
|--------------|-------------------|-------------------|------------------------|--|
| ILC-SPPC1 | 0.5 | 35.6 | 8.44 | 2.51×10^{31} |
| ILC-SPPC2 | 0.5 | 68 | 11.66 | 6.45×10^{31} |
| PWFALC-SPPC1 | 5 | 35.6 | 26.68 | 7.37×10^{30} |
| PWFALC-SPPC2 | 5 | 68 | 36.88 | 1.89×10^{31} |

collider projects, namely the ILC and PWFALC (Plasma Wake Field Accelerator Linear Collider) [46].

In this paper the production potential of the excited electrons at these four electron-proton colliders are investigated using the parameters in the table 2, in which two parameter options (35.6 from the Pre-CDR and 68 TeV) for the energy of the proton beam are used. It is expected that the luminosity values given in this table can be increased at later stages of the project. So, in the analysis part of this work calculations were made using more than one luminosity value for each collider. For such SPPC-based electron-proton colliders suitable detectors have not been designed yet. Thus, this analysis does not include any detector simulation and it is at the parton level.

III. EFFECTIVE LAGRANGIAN, DECAY WIDTHS AND CROSS-SECTIONS

The gauge interaction of a spin-1/2 excited lepton with the ordinary leptons and a gauge boson (γ, Z, W^\pm) is described by following SU(2) \times U(1) invariant Lagrangian [47–50],

$$L = \frac{1}{2\Lambda} \bar{l}_R^* \sigma^{\mu\nu} [fg \frac{\vec{\tau}}{2} \cdot \vec{W}_{\mu\nu} + f'g' \frac{Y}{2} B_{\mu\nu}] l_L + h.c., \quad (1)$$

where l and l^* denote ordinary lepton and the excited lepton, respectively, Λ is the compositeness scale, $\vec{W}_{\mu\nu}$ and $B_{\mu\nu}$ are the field strength tensors, g and g' are the gauge couplings, f and f' are the scaling factors, Y is hypercharge, $\sigma^{\mu\nu} = i(\gamma^\mu\gamma^\nu - \gamma^\nu\gamma^\mu)/2$ where γ^μ are the Dirac matrices, and $\vec{\tau}$ represents the Pauli matrices.

For the excited electrons, three decay modes are possible: radiative decay $e^* \rightarrow e\gamma$, neutral weak decay $e^* \rightarrow eZ$ and charged weak decay $e^* \rightarrow \nu W^-$. Photon channel is preferred in this study because it can be easily detected.

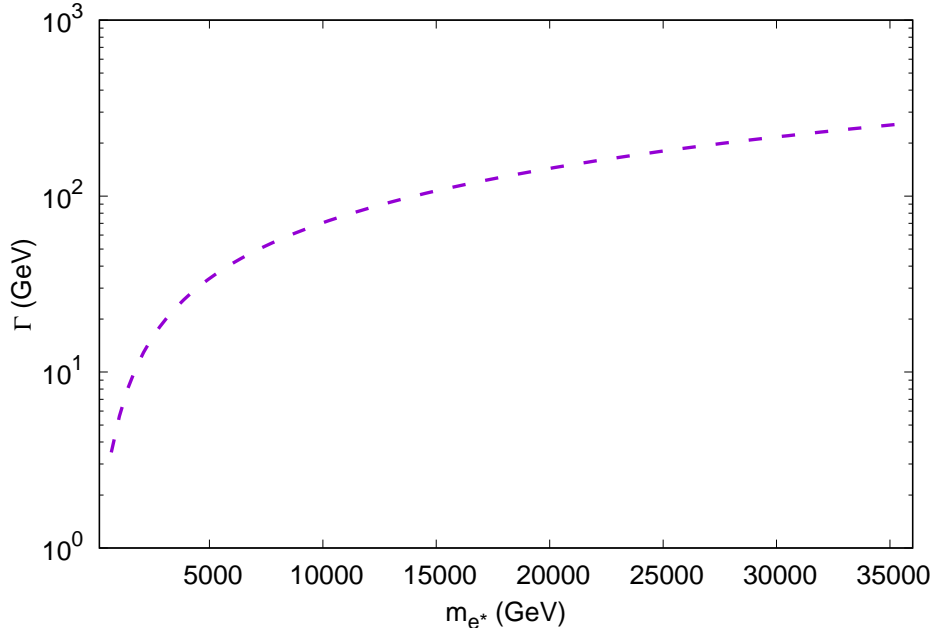


Figure 1: The total decay widths of the excited electron for the energy scale $\Lambda = m_{e^*}$

Neglecting the SM electron mass, the decay widths of the excited electrons for the gauge interactions are given as,

$$\Gamma(l^* \rightarrow lV) = \frac{\alpha m^{*3}}{4\Lambda^2} f_V^2 \left(1 - \frac{m_V^2}{m^{*2}}\right)^2 \left(1 + \frac{m_V^2}{2m^{*2}}\right), \quad (2)$$

where m^* is the mass of the excited electron, f_V is the new electroweak coupling parameter corresponding to the gauge boson V , where $V=W, Z, \gamma$, and $f_\gamma = -(f + f')/2$, $f_Z = (-f \cot \theta_W + f \tan \theta_W)/2$, $f_W = (f/\sqrt{2} \sin \theta_W)$, where θ_W is the weak mixing angle, and m_V is the mass of the gauge boson.

For the numerical calculations we have used the program CALCHEP [51] for signal event production and MADGRAPH [52] for background event production, which are high-energy simulation programmes. We present the total decay widths of the excited electron in Figure 1 for the energy scale $\Lambda = m_{e^*}$. Figure 2 shows the total cross-sections for the excited electron production at the SPPC-based four electron-proton colliders, using the CTEQ6L1 parton distribution functions [53].

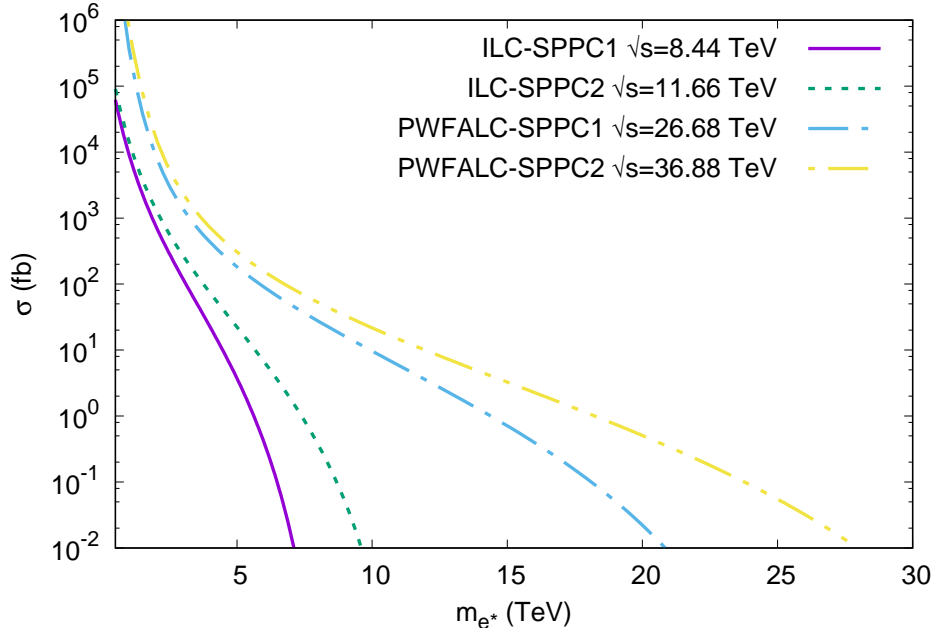


Figure 2: The total production cross-sections of the excited electrons with respect to its mass at the SPPC-based electron-hadron colliders with various center-of-mass energies for $\Lambda = m_{e^*}$ and the coupling $f = f' = 1$.

IV. SIGNAL AND BACKGROUND ANALYSIS

We have analyzed in this section the potentials of the future lepton-hadron colliders to search for the excited electrons through the single production process $ep \rightarrow e^*X$ with subsequent decays of the excited electrons into an electron and photon. Thus, we consider the process $ep \rightarrow e, \gamma, j$ for signal and background, where j represents jets that are composed of quarks ($u, \bar{u}, d, \bar{d}, c, \bar{c}, s, \bar{s}, b, \bar{b}$). The subprocesses are $eq(\bar{q}) \rightarrow e\gamma q(\bar{q})$, where q represents quarks (u, d, c, s, b) and \bar{q} represents anti-quarks ($\bar{u}, \bar{d}, \bar{c}, \bar{s}, \bar{b}$). The Feynman diagrams for the signal process are shown in Fig.3. We discuss here the differences in the signal and background over some kinematical quantities of final-state particles to assign the kinematical cuts best suited for the discovery of the excited electrons.

There are four electron-proton colliders with different center-of-mass energies. The ILC parameters for the first two (called ILC-SPPC1 and ILC-SPPC2) and the PWFALC parameters for the last two (called PWFALC-SPPC1 and PWFALC-SPPC2) are used according to the Table 2. Thus, in the following sub-sections these colliders are covered under two

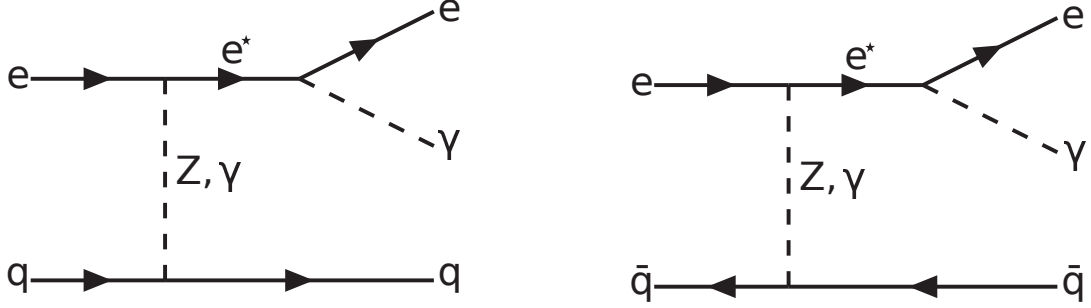


Figure 3: Leading-order Feynman diagrams for the signal process $ep \rightarrow e, \gamma, j$.

categories as ILC-SPPC and PWFALC-SPPC colliders.

ILC-SPPC Colliders

In order to separate the excited electron signals from the background we have firstly applied pre-selection cuts to the transverse momentum of the electron, photon and jets in the final-state as $P_T^{e,\gamma,j} > 20$ GeV. We have generated 10^5 events for both the signal and background, and plotted angular distributions and transverse momentum distributions of the final-state particles using these event files. The event generation for the signal was made for various mass values at the specific intervals starting from 3000 GeV. Because both ILC-SPPC colliders have similar distributions, here's just one of them shown.

Figure 4 shows angular distributions and transverse momentum distributions of the electron and photon in the final-state for the ILC-SPPC collider with $\sqrt{s} = 8.4$ TeV. The pseudorapidity distributions (top-left and bottom-left) of the signal are peaked almost at $\eta = [-1, -2]$ interval for given parameter values ($m_{e^*} = 3000, 5000$ GeV and $\Lambda = m_{e^*}$) of both particles. Since the pseudorapidity is defined as $\eta = -\ln \tan(\theta/2)$, where θ is polar angle, the electrons and photons are of backward, as a result the excited electrons are produced in the backward direction. Also, the separation of the signal and background from each other is very well for all mass values. To reduce the contributions from the background we applied a cut on the pseudorapidity for both particles as $-3 < \eta^e < 0.4$ and $-5 < \eta^\gamma < 0$.

When we look at the transverse momentum distributions in the top-right and bottom-right panels of the same figure, it is seen that the signal and background are still separated from each other for both particles. Thus, we applied a cut at 300 GeV (for electron) and 400 GeV (for photon) to reduce the background. These cuts do not affect the signal too much.

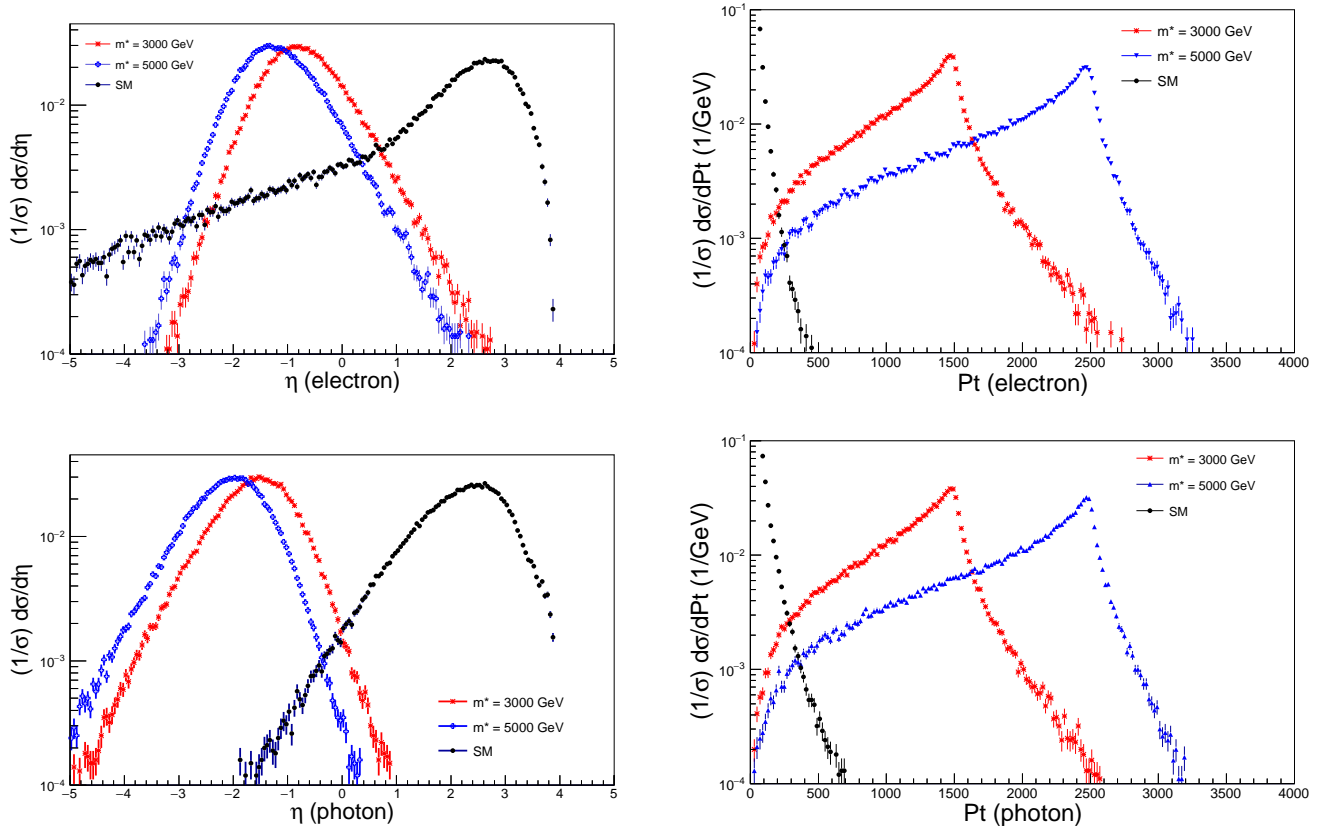


Figure 4: Some kinematical distributions of particles in the final-state for the ILC-SPPC collider with $\sqrt{s} = 8.4$ TeV. In the left-top and right-top panels we show normalized pseudorapidity and transverse momentum distributions of the electron, respectively. The similar distributions for photon are shown in the lower panels. All distributions contain statistical errors.

As for the ILC-SPPC collider with $\sqrt{s} = 11.6$ TeV (ILC-SPPC2), similar distributions in large part have been obtained. Similar analyzes have been made and the kinematical cuts best suited for discovery of the excited electrons have been determined as $-3 < \eta^e < 1$, $-5 < \eta^\gamma < 0.2$, $p_T^e > 300$, $p_T^\gamma > 400$ GeV.

We calculated the selection efficiencies to see how the applied discovery cuts affected the signal and the background. As can be seen from Table 3 and 4, the efficiency values for the signal are greater than 90% for both ILC-SPPC colliders. This shows that the discovery cuts applied have very little effect on the signal. As for the background, the efficiency values are close to zero because the background is drastically reduced. These tables also show the cross-sections before and after the discovery cuts for both colliders.

Another way to see the effect of the discovery cuts applied is to draw invariant mass

Table III: The efficiencies of the standard model background and of our signature after the application of all discovery cuts for the ILC-SPPC collider with $\sqrt{s} = 8.4$ TeV.

| | | σ before cut (fb) | σ after cut (fb) | efficiency (ϵ) |
|-----------------|------|--------------------------|-------------------------|---------------------------|
| background | | 22100 | 10.608 | 0.00048 |
| m_{e^*} (GeV) | 3000 | 12.8 | 11.5 | 0.89 |
| | 3500 | 5.99 | 5.54 | 0.92 |
| | 4000 | 2.78 | 2.61 | 0.93 |
| | 4500 | 1.24 | 1.18 | 0.95 |
| | 5000 | 0.52 | 0.50 | 0.96 |
| | 5500 | 0.19 | 0.18 | 0.94 |
| | 6000 | 0.064 | 0.062 | 0.96 |
| | 6500 | 0.017 | 0.016 | 0.94 |
| | 7000 | 0.0033 | 0.0032 | 0.96 |
| | 7500 | 0.00047 | 0.00045 | 0.95 |
| | 8000 | 0.000107 | 0.000101 | 0.94 |

distributions for both the signal and background. Figure 5 shows the invariant mass distributions of the excited electron and the corresponding background after the application of all discovery cuts for the ILC-SPPC colliders. It is clearly seen from this figure that the background curves are below the signal peaks for the both colliders.

In order to calculate the statistical significance (SS) of the expected signal yield, we have used the formula of

$$SS = \sqrt{2 \left[(S + B) \ln \left(1 + \left(\frac{S}{B} \right) \right) - S \right]}, \quad (3)$$

where S and B denote event numbers of the signal and background, respectively. In Fig. 6 we show the contour plots of $S = 2$ (2σ -exclusion), 3 (3σ -observation) and 5 (5σ -discovery) in the parameter space (L, m^*) , where L is integrated luminosity of the collider, for both ILC-SPPC colliders. We consider a scan of the parameter space (L, m^*) within the range $L \in [1, 100] \text{ fb}^{-1}$ with step of 10 fb^{-1} . In these distributions the regions below the $S = 5$ curve are excluded.

Table IV: The efficiencies of the standard model background and of our signature after the application of all discovery cuts for the ILC-SPPC collider with $\sqrt{s} = 11.6$ TeV.

| | | σ before cut (fb) | σ after cut (fb) | efficiency (ϵ) |
|-----------------|---------|--------------------------|-------------------------|---------------------------|
| background | | 29600 | 15.98 | 0.00053 |
| m_{e^*} (GeV) | 3000 | 27.5 | 26.04 | 0.94 |
| | 3500 | 15.1 | 14.51 | 0.96 |
| | 4000 | 8.53 | 8.27 | 0.96 |
| | 4500 | 4.94 | 4.82 | 0.97 |
| | 5000 | 2.89 | 2.82 | 0.97 |
| | 5500 | 1.62 | 1.58 | 0.97 |
| | 6000 | 0.937 | 0.917 | 0.97 |
| | 6500 | 0.499 | 0.489 | 0.97 |
| | 7000 | 0.262 | 0.256 | 0.97 |
| | 7500 | 0.129 | 0.125 | 0.96 |
| | 8000 | 0.059 | 0.058 | 0.98 |
| | 8500 | 0.025 | 0.024 | 0.96 |
| | 9000 | 0.0093 | 0.0089 | 0.95 |
| | 9500 | 0.0029 | 0.0028 | 0.96 |
| 10000 | 0.00078 | 0.00074 | 0.94 | |

PWFALC-SPPC Colliders

If the excited electrons had not been observed at the ILC-SPPC colliders, they would have been explored up to the mass of 26.6 TeV and 36.8 TeV at the PWFALC-SPPC1 and PWFALC-SPPC2 colliders, respectively. To separate the signal from the background we have required kinematical cuts $P_T^{e,\gamma,j} > 20$ GeV, as for the ILC-SPPC colliders. Figure 7 shows angular distributions and transverse momentum distributions of the electron and photon in the final-state for the PWFALC-SPPC collider with $\sqrt{s} = 26.6$ TeV. It has been seen that the pseudorapidity distributions (top-left and bottom-left) with low mass values like 3000 GeV of the signal are in the positive region compared to those of the ILC-SPPC colliders. Therefore, some of the excited electrons in these colliders are produced in the

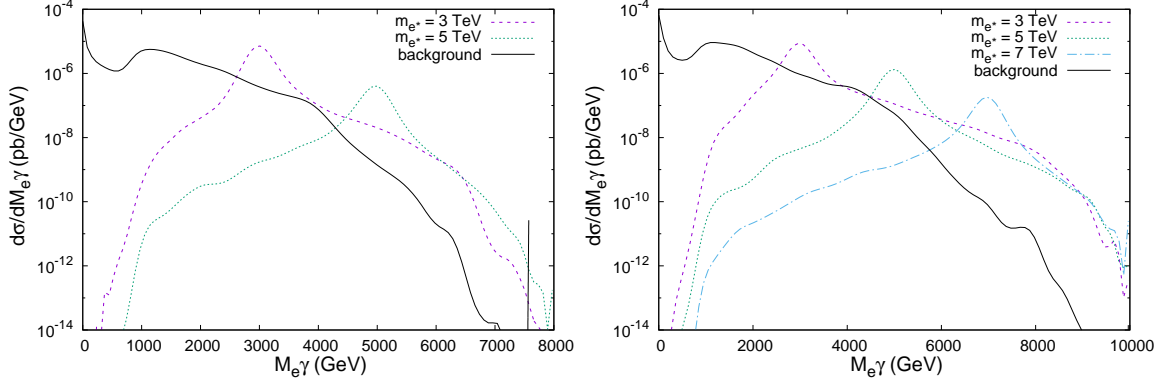


Figure 5: The distributions in the invariant mass of the excited electron signal and the corresponding background for the ILC-SPPC colliders. The left panel shows the distributions at the collider with $\sqrt{s} = 8.4$ TeV for the excited electron masses of 3 and 5 TeV, and the right panel shows the distributions at the collider with $\sqrt{s} = 11.6$ TeV for the excited electron masses of 3,5 and 7 TeV.

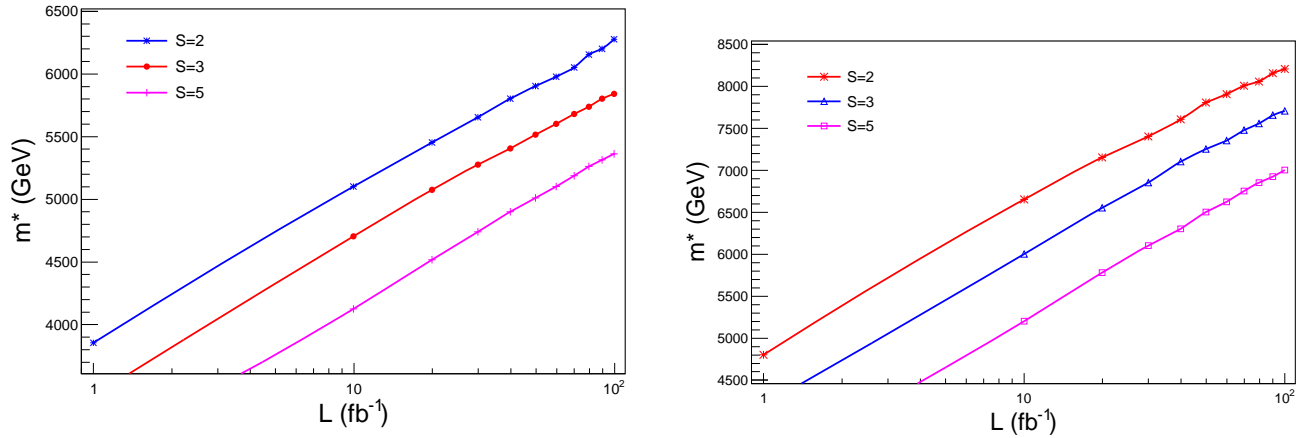


Figure 6: Contour maps of the statistical significance for $S=2, 3$ and 5 in the parameter space (L, m^*) for the ILC-SPPC collider with $\sqrt{s} = 8.4$ (left) and 11.6 TeV (right).

forward direction. On the other hand, the signal and background curves are well separated from each other for all mass values. To greatly reduce the effect of the background we applied a cut on these distributions for both particles as $-2 < \eta^e < 3.2$ and $-5 < \eta^\gamma < 2.4$. The pseudorapidity cuts for the PWFALC-SPPC collider with $\sqrt{s} = 36.8$ TeV that has similar distributions are $-2 < \eta^e < 3$ and $-5 < \eta^\gamma < 2.5$.

In the transverse momentum distributions (top-right and bottom-right) it has been seen that the signal and the background are again separated from each other in a good way. The

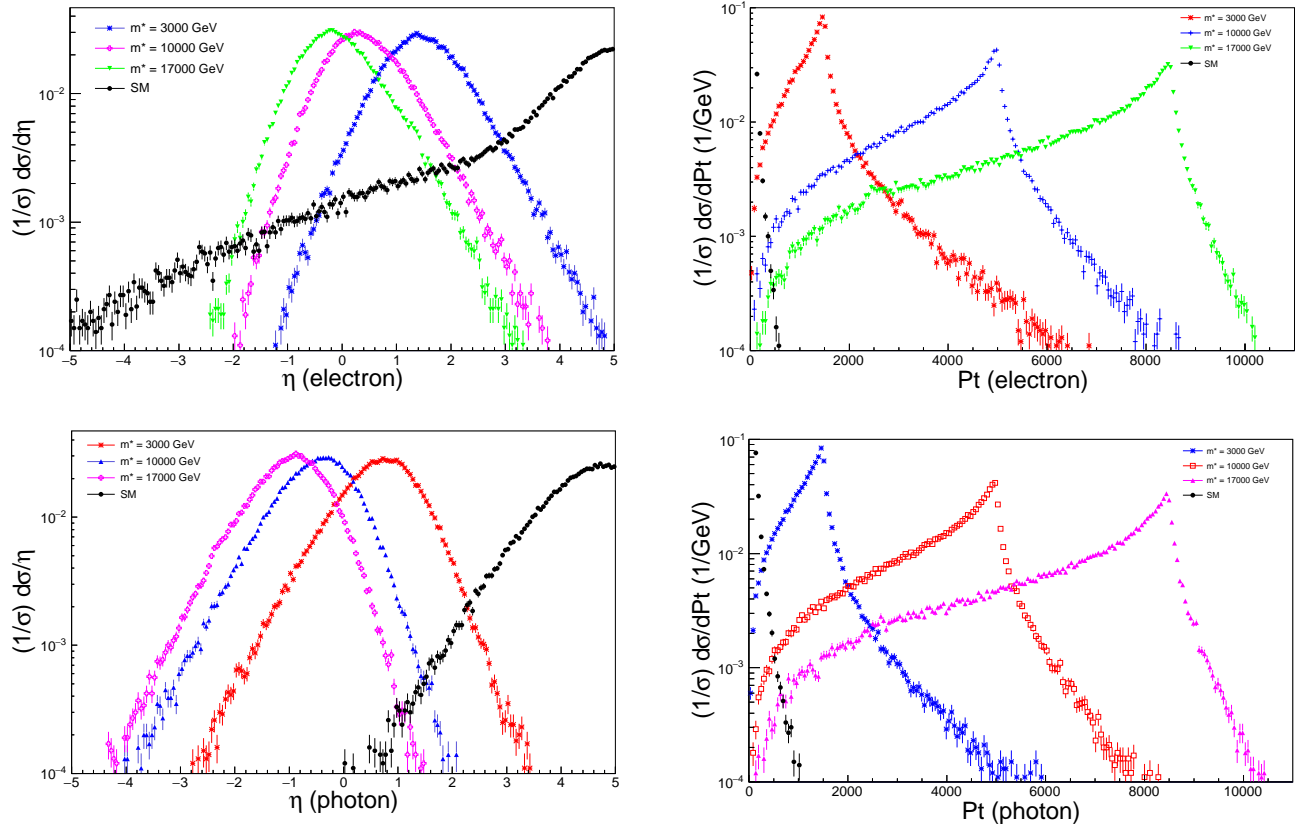


Figure 7: Some kinematical distributions of particles in the final-state for the PWFALC-SPPC collider with $\sqrt{s} = 26.6$ TeV. In the left-top and right-top panels we show normalized pseudorapidity and transverse momentum distributions of the electron, respectively. The similar distributions for photon are shown in the lower panels. All distributions contain statistical errors.

transverse momentum cuts for these distributions are determined as $p_T^e > 400$, $p_T^\gamma > 500$ GeV for the both colliders. Table 5 and 6 show the selection efficiencies after the application of all kinematical cuts for both colliders. These tables show that the applied cuts drastically reduce the background and have little effect on the signal.

When we examine the invariant mass distributions, shown in Fig.8 for both colliders, obtained after applying the cuts it has been seen that the signal peaks are above the background curve.

And finally we plot the statistical significance curves of the expected signal in the parameter space (L, m^*) as shown in Fig. 9 for both colliders. The areas under the curve $S = 5$ are the mass values excluded by the collider.

Table V: The efficiencies of the standard model background and of our signature after the application of all discovery cuts for the PWFALC-SPPC collider with $\sqrt{s} = 26.6$ TeV.

| | | σ before cut (fb) | σ after cut (fb) | efficiency (ϵ) |
|-----------------|----------|--------------------------|-------------------------|---------------------------|
| background | | 60100 | 15.62 | 0.00025 |
| m_{e^*} (GeV) | 3000 | 108 | 98.9 | 0.91 |
| | 4000 | 42 | 40.1 | 0.95 |
| | 5000 | 20 | 19.4 | 0.97 |
| | 6000 | 10.5 | 10.3 | 0.98 |
| | 7000 | 5.9 | 5.8 | 0.98 |
| | 8000 | 3.4 | 3.3 | 0.97 |
| | 9000 | 2 | 1.9 | 0.95 |
| | 10000 | 1.2 | 1.19 | 0.99 |
| | 11000 | 0.792 | 0.786 | 0.99 |
| | 12000 | 0.491 | 0.488 | 0.99 |
| | 13000 | 0.299 | 0.297 | 0.99 |
| | 14000 | 0.178 | 0.177 | 0.99 |
| | 15000 | 0.104 | 0.103 | 0.99 |
| | 16000 | 0.0586 | 0.0583 | 0.99 |
| | 17000 | 0.032 | 0.031 | 0.96 |
| | 18000 | 0.0163 | 0.0162 | 0.99 |
| | 19000 | 0.00789 | 0.00784 | 0.99 |
| 20000 | 0.00352 | 0.00349 | 0.99 | |
| 21000 | 0.00139 | 0.00138 | 0.99 | |
| 22000 | 0.000489 | 0.000485 | 0.99 | |

V. CONCLUSION

In this work, the production potential of the excited electrons predicted by the composite models at the four SPPC-based lepton-hadron colliders, namely ILC-SPPC1 ($\sqrt{s} = 8.44$ TeV), ILC-SPPC2 ($\sqrt{s} = 11.66$ TeV), PWFALC-SPPC1 ($\sqrt{s} = 26.68$ TeV) and PWFALC-SPPC2 ($\sqrt{s} = 36.88$ TeV) has been searched. In the all simulations it is assumed that

Table VI: The efficiencies of the standard model background and of our signature after the application of all discovery cuts for the PWFALC-SPPC collider with $\sqrt{s} = 36.8$ TeV.

| | | σ before cut (fb) | σ after cut (fb) | efficiency (ϵ) |
|-----------------|----------|--------------------------|-------------------------|---------------------------|
| background | | 78400 | 40.76 | 0.00051 |
| m_{e^*} (GeV) | 3000 | 172.6 | 158.2 | 0.91 |
| | 5000 | 33.2 | 32.2 | 0.96 |
| | 7000 | 10.6 | 10.4 | 0.98 |
| | 9000 | 4.33 | 4.28 | 0.98 |
| | 11000 | 1.97 | 1.95 | 0.98 |
| | 13000 | 0.959 | 0.952 | 0.99 |
| | 15000 | 0.473 | 0.470 | 0.99 |
| | 17000 | 0.2309 | 0.2294 | 0.99 |
| | 19000 | 0.1109 | 0.1100 | 0.99 |
| | 21000 | 0.0515 | 0.0510 | 0.99 |
| | 23000 | 0.0221 | 0.0218 | 0.98 |
| | 25000 | 0.00842 | 0.00831 | 0.98 |
| | 27000 | 0.00282 | 0.00277 | 0.98 |
| | 29000 | 0.000778 | 0.000763 | 0.98 |
| 31000 | 0.000163 | 0.000159 | 0.97 | |

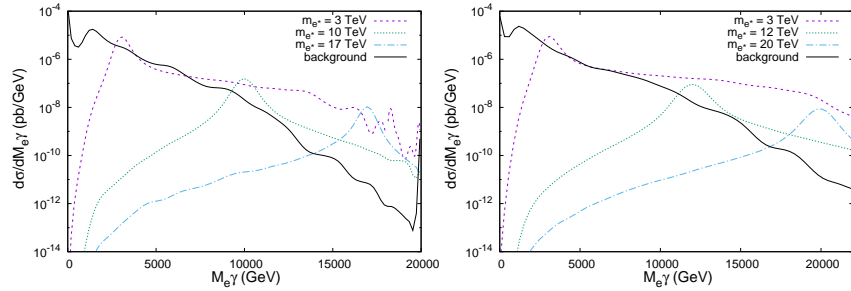


Figure 8: The distributions in the invariant mass of the excited electron signal and the corresponding background for the PWFALC-SPPC colliders. The left panel shows the distributions at the collider with $\sqrt{s} = 26.6$ TeV for the excited electron masses of 3, 10 and 17 TeV, and the right panel shows the distributions at the collider with $\sqrt{s} = 36.8$ TeV for the excited electron masses of 3,12 and 20 TeV.

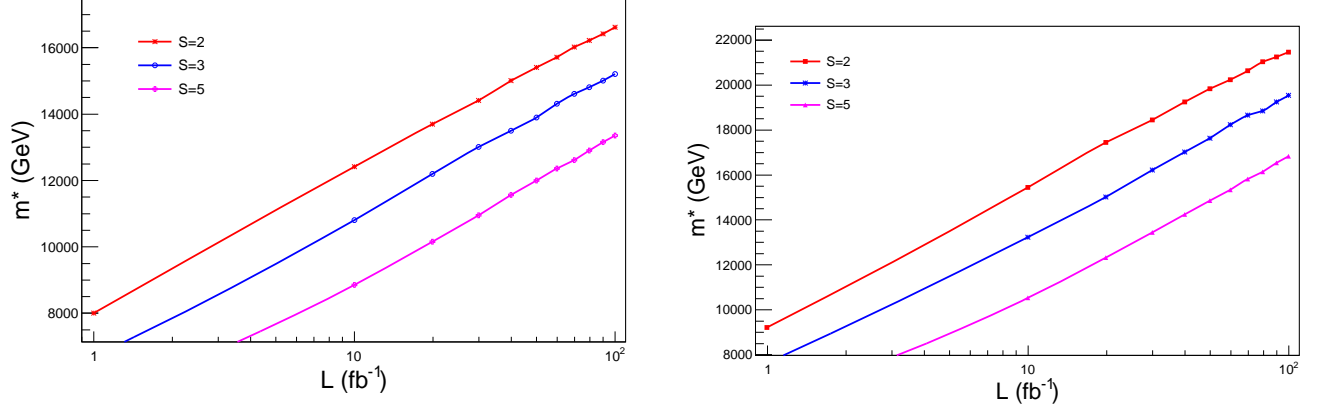


Figure 9: Contour maps of the statistical significance for $S=2, 3$ and 5 in the parameter space (L, m^*) for the PWFALC-SPPC collider with $\sqrt{s} = 26.6$ (left) and 36.8 TeV (right).

the energy scale is $\Lambda = m_{e^*}$ and the coupling parameter is $f = f' = 1$. In the analysis, kinematical cuts required for the discovery of the excited electrons were determined for the particles in final-state. To see how these cuts affect the signal and the background, the values of selection efficiency are calculated and the invariant mass distributions were drawn. Finally the statistical significance values of the expected signal yield were calculated using different integrated luminosity values within the range $L \in [1, 100] \text{ fb}^{-1}$ with step of 10 fb^{-1} . The curves indicating the mass limits for exclusion, observation and discovery of the excited electrons have been plotted in the parameter space (L, m^*). For example, mass limit of observation of the excited electron at the PWFALC-SPPC2 collider that has the highest center-of-mass energy is 16.8 TeV for the integrated luminosity $L = 100 \text{ fb}^{-1}$. Smaller mass values are excluded.

As a result, the future SPPC-based lepton-hadron colliders will play an important role in the investigation of the excited electrons.

Conflict of Interest

The author declares that he has no conflict of interest.

Acknowledgments

I would like to thank Dr. A. Ozansoy for support of the model file. This work has been supported by the Scientific and Technological Research Council of Turkey (TÜBİTAK) under the Grant no. 114F337.

- [1] ATLAS Collaboration, “Observation of a new particle in the search for the Standard Model Higgs boson with the ATLAS detector at the LHC”, *Phys. Lett. B*, 716 (1), 1-29 (2012).
- [2] CMS Collaboration, “Observation of a new boson at a mass of 125 GeV with the CMS experiment at the LHC”, *Phys. Lett. B*, 716 (1), 30-61 (2012).
- [3] S. Weinberg, “Implications of dynamical symmetry breaking”, *Phys. Rev. D*, 13, 974-996 (1976).
- [4] L. Susskind, “Dynamics of spontaneous symmetry breaking in the Weinberg-Salam theory”, *Phys. Rev. D*, 20, 2619-2625 (1979).
- [5] H. Georgi and S. L. Glashow, “Unity of all elementary-particle forces”, *Phys. Rev. Lett.*, 32, 438 (1974).
- [6] J. C. Pati and A. Salam, “Lepton number as the fourth color”, *Phys. Rev. D*, 10, 275 (1974).
- [7] Y. A. Golfand and E. P. Likhtman, “Extension of the algebra of Poincaré group generators and violation of P invariance”, *JETP Lett.*, 13, 323 (1971).
- [8] I.A. D’Souza and C.S. Kalman, *PREONS: Models of leptons, quarks and gauge bosons as composite objects*, World Scientific Publishing, 1992.
- [9] H. Terazawa, Y. Chikashige and K. Akama, “Unified model of the Nambu-Jona-Lasinio type for all elementary-particle forces”, *Phys. Rev. D*, 15 (2), 480 (1977).
- [10] H. Terazawa, “Subquark model of leptons and quarks”, *Phys. Rev. D*, 22 (1), 184 (1980).
- [11] H. Terazawa, M. Yasue, K. Akama and M. Hayashi, “Observable effects of the possible substructure of lepton and quarks”, *Phys. Lett. B*, 112 (4-5), 387-392 (1982).
- [12] H. Terazawa, “A fundamental theory of composite particles and fields”, *Phys. Lett. B*, 133 (1-2), 57-60 (1983).
- [13] H. Fritzsch and G. Mandelbaum, “Weak interactions as manifestations of the substructure of leptons and quarks”, *Phys. Lett. B*, 102 (5), 319-322 (1981).
- [14] O.W. Greenberg and J. Sucher, “A quantum structure dynamic model of quarks, leptons, weak

- vector bosons and Higgs mesons”, *Phys. Lett. B*, 99 (4), 339-343 (1981).
- [15] H. Harari, “A schematic model of quarks and leptons”, *Phys. Lett. B*, 86 (1), 83-86 (1979).
- [16] M.A. Shupe, “A composite model of leptons and quarks”, *Phys. Lett. B*, 86 (1), 87-92 (1979).
- [17] L. F. Abbott and E. Farhi, “Are the weak interactions strong?”, *Phys. Lett. B*, 101(1-2), 69-72 (1981).
- [18] R. Leonardi, L. Alunni, F. Romeo, L. Fano and O. Panella, “Hunting for heavy composite Majorana neutrinos at the LHC”, *Eur. Phys. J. C.*, 76, 593 (2016).
- [19] S. Biondini, O. Panella, G. Pancheri, Y. N. Srivastava and L. Fano, “Phenomenology of excited doubly charged heavy leptons at LHC”, *Phys. Rev. D*, 85, 095018 (2012).
- [20] R. Leonardi, O. Panella and L. Fano, “Doubly charged heavy leptons at LHC via contact interactions”, *Phys. Rev. D*, 90, 035001 (2014).
- [21] M. Köksal, “Analysis of excited neutrinos at the CLIC”, *Int. J. Mod. Phys.*, A29, 1450138 (2014).
- [22] A. Ozansoy, V. Ari and V. Cetinkaya, “Search for excited spin-3/2 neutrinos at LHeC”, *Adv. High Energy Phys.*, 2016, 1739027 (2016).
- [23] A. Caliskan, S.O. Kara and A. Ozansoy, “Excited muon searches at the FCC-based muon-hadron colliders”, *Adv. High Energy Phys.*, 2017, 1540243 (2017).
- [24] A. Caliskan, “Excited neutrino search potential of the FCC-based electron-hadron colliders”, *Adv. High Energy Phys.*, 2017, 4726050 (2017).
- [25] L3 Collaboration, “Search for excited leptons at LEP”, *Phys. Lett. B*, 568,1 (2003).
- [26] H1 Collaboration, “Search for excited electrons in ep collisions at HERA”, *Phys. Lett. B*, 666, 2 (2008).
- [27] D0 Collaboration, “Search for excited electrons in $p\bar{p}$ collision at $\sqrt{s} = 1.96$ TeV”, *Phys. Rev. D*, 77, 091102, (2008).
- [28] ATLAS Collaboration, “Search for excited electrons and muons $\sqrt{s} = 8$ TeV proton-proton collisions with the ATLAS detector”, *New J. Phys.*, 15, 093011 (2013).
- [29] CMS Collaboration, “Search for excited leptons in $l\gamma$ final states in proton-proton collisions at $\sqrt{s} = 13$ TeV”, *JHEP*, 2019, 15 (2019).
- [30] M. Tanabashi, K. Hagiwara, K. Hikasa et al., (Particle Data Group), “The review of particle physics”, *Phys. Rev. D*, 98, 030001 (2018).
- [31] C. Adolphsen, M. Barone, B. Barish et al., “The International Linear Collider Technical Design

- Report - Volume 3.2”, e-print, arXiv:1306.6328 [physics.acc-ph] (2013).
- [32] J.P. Delahaye, C. Ankenbrandt, A. Bogacz et al., “Enabling intensity and energy frontier science with a muon accelerator facility in the U.S., e-print, arXiv:1308.0494 [physics.acc-ph] (2014).
- [33] LHeC Project Web Page: <http://lhec.web.cern.ch>.
- [34] CLIC Collaboration, “The CLIC programme: Towards a staged e^+e^- linear collider exploring the terascale”, CLIC Conceptual Design Report, CERN-2012-005, CERN, Geneva (2012).
- [35] FCC Project Web Page: <https://fcc.web.cern.ch>.
- [36] TLEP Project Web Page: <https://tlep.web.cern.ch>.
- [37] FCC Collaboration, “Future Circular Collider Study Volume 1: Physics Opportunities”, Conceptual Design Report, preprint edited by M. Mangano et al. CERN accelerator reports, CERN-ACC-2018-0056, submitted to Eur. Phys. J. C, Geneva (2018).
- [38] FCC Collaboration, “Future Circular Collider Study Volume 2: The Lepton Collider (FCC-ee)”, Conceptual Design Report, preprint edited by M. Benedikt et al. CERN accelerator reports, CERN-ACC-2018-0057, submitted to Eur. Phys. J. ST, Geneva (2018).
- [39] FCC Collaboration, “Future Circular Collider Study Volume 3: The Hadron Collider (FCC-hh)”, Conceptual Design Report, preprint edited by M. Benedikt et al. CERN accelerator reports, CERN-ACC-2018-0058, submitted to Eur. Phys. J. ST, Geneva (2018).
- [40] FCC Collaboration, “Future Circular Collider Study Volume 4: The High Energy LHC (HE-LHC)”, Conceptual Design Report, preprint edited by F. Zimmermann et al. CERN accelerator reports, CERN-ACC-2018-0059, submitted to Eur. Phys. J. ST, Geneva (2018).
- [41] The CEPC-SPPC Study Group, CEPC-SPPC Preliminary Conceptual Design Report, Volume I - Physics & Detector, IHEP-CEPC-DR-2015-01, March (2015).
- [42] CEPC Study Group, “CEPC Conceptual Design Report: Volume 1 - Accelerator”, Conceptual Design Report, IHEP-CEPC-DR-2018-01, IHEP-AC-2018-01, arXiv preprint: 1809.00285 (2018).
- [43] CEPC Study Group, “CEPC Conceptual Design Report: Volume 2 - Physics & Detector”, Conceptual Design Report, HEP-CEPC-DR-2018-02, IHEP-EP-2018-01, IHEP-TH-2018-01, arXiv preprint: 1811.10545 (2018).
- [44] F. Su, J. Gao, Y. Chen et al., “SPPC Parameter Choice and lattice design”, Proceedings of IPAC2016, Busan, Korea, 1400-1402 (2016).

- [45] A. C. Canbay, U. Kaya, B. Ketenoglu, B. B. Oner and S. Sultansoy, “SppC based energy frontier lepton-hadron colliders: Luminosity and physics”, *Adv. High Energy Phys.*, 2017, 4021493 (2017).
- [46] J. P. Delahaye, E. Adli, S. J. Gessner et al., “A beam driven plasma-wakefield linear collider from Higgs factory to multi-TeV”, *Proceedings of IPAC2014, Dresden, Germany*, 3791 (2014).
- [47] K. Hagiwara, D. Zeppenfeld and S. Komamiya, “Excited lepton production at LEP and HERA”, *Z. Phys. C*, 29, 115 (1985).
- [48] U. Baur, M. Spira and P. M. Zerwas, “Excited-quark and -lepton production at hadron colliders”, *Phys. Rev. D*, 42, 815 (1990).
- [49] F. Boudjema and A. Djouadi, “Looking for the LEP at LEP. The excited neutrino scenario”, *Phys. Lett. B*, 240, 485-491 (1990).
- [50] F. Boudjema, A. Djouadi and J. L. Kneur, “Excited fermions at e^+e^- and ep colliders”, *Z. Phys. C*, 57, 425 (1993).
- [51] A. Belyayev, N. D. Christensen and A. Pukhov, “CalcHEP 3.4 for collider physics within and beyond the Standard Model”, *Comput. Phys. Commun.*, 184, 1729 (2013).
- [52] J. Alwall, R. Frederix, S. Frixione et al., “The automated computation of tree-level and next-to-leading order differential cross sections, and their matching to parton shower simulations”, *Journal of High Energy Physics*, 079 (2014).
- [53] D. Stump, J. Huston, J. Pumplin et al., “Inclusive jet production, parton distributions and the search for new physics”, *JHEP*, 0310, 046 (2003).